

THIS ISSUE

Western Nanofabrication Facility at Discovery 2009	1
Poster Contest	1
Study of Interaction of Metal Ions with DNA Films	2

For More Information Visit Our Website

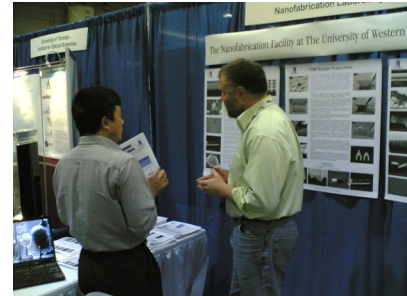
www.uwo.ca/fab

- Examples of work
- Contact Information
- Facilities Information
- How to become a user of the facility
- Services provided
- Subscribe to our newsletter

Questions & Comments?
Send them to:
nanofab@uwo.ca

Western Nanofabrication Facility at Discovery 2009

The annual OCE (Ontario Centres of Excellence) showcase took place at the Metro Toronto Convention Centre over Monday 11th and Tuesday 12th May. The showcase with the theme "Future Ready" was a big hit this year with over 2,200 delegates and 300 exhibitors. The UWO Nanofabrication Facility had a booth at the showcase. The team consisted of Prof. Bernie Kraatz, Todd Simpson and Rick Glew. Arriving by train, we put up the display in time for the evening opening reception on Monday. After a night at a Hotel we were back for breakfast and manning the booth. With a team of three it gave us the opportunity of listening to the numerous talks and panel discussions. Also at the showcase were UWO groups from Engineering, SHARCNET and Surface Science. The team made numerous contacts with students, business representatives, government agencies and international organizations. While we were tearing down at 5 o'clock delegates were still queuing to ask questions, but we had a train to catch.



Nanofabrication Poster Contest

We need "mini-posters" describing work done in the Nanofabrication Facility to use on our webpage and in promotional material.

Submit a one page report on any component of your research that has utilized the Nanofabrication Facility and earn up to \$125.

Multiple entries are welcome, provided they describe different projects.

Submissions must include:

- 1) Name & affiliation
- 2) Names of collaborators & supervisor.
- 3) An introductory paragraph describing the research project.
- 4) A minimum of one figure with a caption.
- 5) A paragraph describing the work performed in the Nanofabrication Facility.
- 6) References to any publications and presentations resulting from the work.

Formatted figures and text should fit one 8.5x11 page.

This offer is open to all current and former users of the Nanofabrication Facility.

Qualified submissions will earn a \$25 gift card to the Western book & computer store or Chapters.

In addition, all entries will be entered into a competition for a \$100 prize and a framed certificate. The judges will be looking for projects that demonstrate innovative use of the Nanofabrication Facility. Winning entries will be featured in the NanoWestern newsletter.

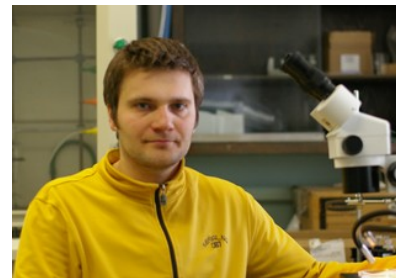
Email your submissions to nanofab@uwo.ca

Study of Interaction of Metal Ions with DNA Films



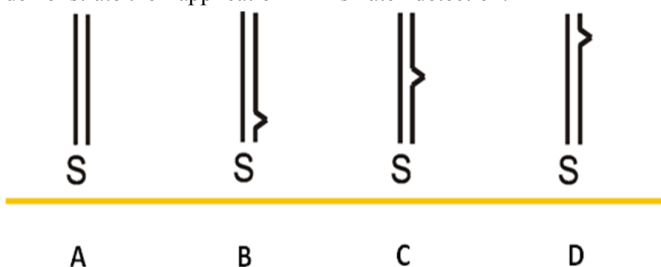
**Xiaomin Bin, Piotr Michal Diakowski
and Heinz-Bernhard Kraatz**

Department of Chemistry
University of Western Ontario
London, Ontario, Canada



The interactions of metal ions with DNA have been investigated extensively and are known to alter the DNA's structure and function.¹ The DNA has four different principal binding sites for metal ions: the negatively charged phosphate backbone, the ribose hydroxyls, the base ring nitrogens, and the exocyclic base keto groups. Alkali and alkaline earth metal cations prefer to bind to the phosphate groups along the backbone of DNA, which essentially reduces the electrostatic repulsion between the strands. Transition metal ions can interact with several sites. In addition to phosphate binding, there are examples in the literature of metal interactions with nucleobases involving the N7 of purines or the N3 of pyrimidines.² In ds-DNA, such coordination tends to cause changes in the structure of the double helix. The interaction of metal ions with ds-DNA films has drawn more attention recently due to its application in the electrochemical detection of single nucleotide mismatches and its application in electrochemical gene chips.^{3,4}

We have shown before that the addition of Zn^{2+} ions causes significant changes in the electrochemical properties of ds-DNA films and enhances our ability to detect single nucleotide mismatches at ultralow concentrations. In our study, we combine electrochemical impedance spectroscopy (EIS) and scanning electrochemical microscopy (SECM) to evaluate the resistive and capacitive properties of ds-DNA films.⁵ Here we focus on the effects of the divalent transition metal ions Ni^{2+} , Cu^{2+} , Zn^{2+} , Cd^{2+} , Hg^{2+} and demonstrate their application in mismatch detection.



Four different 25-mer ds-DNA **A**, **B**, **C** and **D** as shown in above pictures have been used in this study. Among them, **A** is fully matched sequence; **B**, **C** and **D** are ds-DNA with one single A-C mismatch at position of 6, 13 and 19 counting from the 3' end of the complementary sequence.

The fully matched **A** and one single A-C mismatched ds-DNA **C** have been chosen to form DNA films on gold microelectrode surfaces by incubating the freshly cleaned microelectrodes for 5 days in the fridge (4 °C) with ds-DNA hybridized from equimolar amounts of strands (0.1 mM ds-DNA in 20 mM Tris-ClO₄ buffer at pH 8.6). The ds-DNA films were incubated in 0.3 mM solutions of the corresponding metal perchlorates ($M = Ni^{2+}$, Cu^{2+} , Zn^{2+} , Cd^{2+} , and Hg^{2+}) in 20 mM Tris-ClO₄ buffer (pH 8.6) for at least 6 hours at room temperature (21±2 °C). DNA array on gold wafer was carried out using a spotting robot. Standard printing procedure was used.

The spacing between each spot is 250µm. Pre-hybridized ds-DNA **A**, **B**, **C** and **D** solutions were spotted onto gold substrates, which were prepared by thermal e-beam deposition of chromium (100 Å) followed by gold (1000 Å, 99.99% purity) onto a silicon wafer. To ensure proper humidity, the substrates were placed on top of a moist filter paper inside a Petri dish. The Petri dish was then wrapped with Parafilm and incubated for 48h at 4°C.

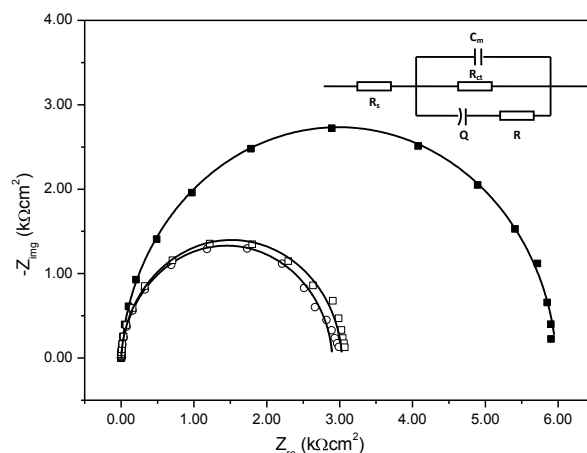


Fig. 1. Nyquist plots (Z_{img} vs. Z_{re}) of a film of ds-DNA assembled from a fully matched 25-mer ds-DNA **A** on gold microelectrode in the absence of metal ions (■), in the presence of metal ions (●) and after extensive washing with 20mM Tris-ClO₄ buffer (pH=8.6) to remove metal ions again (□). Black solid lines were fitting curves by corresponding equivalent circuits. Inset: Equivalent circuits used to fit impedance spectra of ds-DNA monolayer. R_s , solution resistance; C_m , capacitance of monolayer; R_{ct} , charge-transfer resistance; R_x and Q , defects in the monolayer.

The divalent transitional metal cations Ni^{2+} , Cu^{2+} , Zn^{2+} , Cd^{2+} and Hg^{2+} were selected to interact with thin films of 25-mer matched ds-DNA, prepared from strands fully matched **A**. **Fig.1** show the representative Nyquist plots of ds-DNA and its interaction with Zn^{2+} . The figure shows the EIS for ds-DNA films in the absence of metal ions (■), and in the presence of metal ions (●). This was followed by extensive washing of the films with buffer, and their impedance spectra were recorded in buffer in the absence of the corresponding metal ions (□). The experimental data obtained from the impedance measurements was then fitted to an equivalent circuit shown in the inset of **Fig.1**, allowing us to model the observation in terms of resistive and capacitive components and extract numerical values for the circuitry components.

The difference of charge transfer resistance between ds-DNA films in the presence and absence of metal ions ΔR_{ct} is used to evaluate the enhancement

of charge transfer through DNA film by binding different metal ions and is now being used to probe into the differences in the interactions of various metal ions with the ds-DNA film. Fig.2 shows ΔR_{ct} before ($\Delta R_{ct}(1)$) and after washing ($\Delta R_{ct}(2)$) of the ds-DNA films.

The divalent transitional metal cations exhibit significantly different behaviors. The value of $\Delta R_{ct}(1)$ decreases in the following order: $Hg^{2+} > Cd^{2+} > Ni^{2+} > Cu^{2+} > Zn^{2+}$. Washing of the metallated films with buffer provides a picture of how persistent the metal-DNA interactions are. We were surprised to find that Hg^{2+} can be washed away completely and after washing the value of R_{ct} is close to that of unmetallated ds-DNA. Our experimental finding shows that for Hg^{2+} , the highest $\Delta R_{ct}(1)$ value was observed for any of the transitional metal cations. The DNA employed in this study

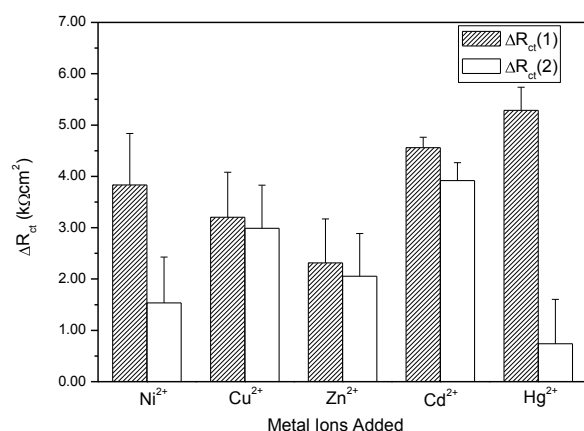


Fig.2. R_{ct} changes (ΔR_{ct}) as a function of metal ions. $\Delta R_{ct}(1)$ represents the difference in the charge transfer resistance R_{ct} observed in films of ds-DNA in the presence and absence of metal ions. $\Delta R_{ct}(2)$ represents the difference of R_{ct} observed in films of ds-DNA after exposure to metal ions before and after rinsing with buffer to remove the metal ions. Error bars represent the standard deviation and are derived from a minimum of five electrodes.

offers a number of potential Hg^{2+} binding sites. Our studies show that Hg^{2+} can be removed from the ds-DNA film, resulting in a value for $\Delta R_{ct}(2)$ that is essentially unchanged from that of unmetallated ds-DNA films. This eliminates the possibility of interaction of Hg^{2+}

ions with the gold thiol bond which would result in film decomposition. Next, it was surprising to find that upon washing a significant amount of Ni^{2+} is lost, resulting in a significant reduction of $\Delta R_{ct}(2)$. Cu^{2+} , Zn^{2+} , and Cd^{2+} display strong and persistent interactions with ds-DNA. The values of ΔR_{ct} before and after extensive washing remain virtually unchanged.

Considering that the interaction of metal ions with DNA involves substitution of coordinated water molecules, the free energy of hydration $-\Delta G_{Hydration}$ of the metal ions is one of the contributing factors to the observed ordering and our data support this and show an inverse relationship between $\Delta G_{solv.}$ and $\Delta R_{ct}(1)$ for the divalent metal ions.

Single mismatched ds-DNA was prepared by hybridization of strands C in a suitable buffer at pH 8.6. This ds-DNA contains an A-C mismatch in position 13. Next, thin films on gold were prepared by incubating gold microelectrodes in a buffered solution of the hybridized ds-DNA. The interaction of metal cations Zn^{2+} , Cd^{2+} and Hg^{2+} with mismatched DNA was evaluated by EIS, and the results were compared with those obtained for films of matched ds-DNA. The corresponding R_{ct} values are summarized in Table 1. First, the charge transfer resistance R_{ct} is smaller for mismatched ds-DNA compared to matched ds-DNA. We rationalize this by additional disorder present in the mismatched films which enables better penetration of the anionic redox probe into the ds-DNA films.

Furthermore R_{ct} for mismatched ds-DNA is significantly lower in the presence of metal ions compared no metal ions being present. However, the decrease is less than that for fully matched ds-DNA films. The difference in the ΔR_{ct} values was used in the detection of single-nucleotide mismatches. The use of ΔR_{ct} was attractive from an application perspective because different electrode morphologies can yield different impedances but the comparative impedance measurements between DNA in the presence and absence of metal ions are reproducible and eliminate the need to evaluate surface variations. For all metal cations, ΔR_{ct} values of matched ds-DNA film are larger than those of single mismatched ds-DNA films. The difference of ΔR_{ct} between matched and mismatched ds-DNA for the four different metal ions ($\Delta\Delta R_{ct}$) is summarized in Table 1. It shows that the $\Delta\Delta R_{ct}$ is the largest for Hg^{2+} and that in fact the $\Delta\Delta R_{ct}$ for Zn^{2+} is the smallest of the metal ions tested. Larger $\Delta\Delta R_{ct}$ values indicate that in fact Hg^{2+} might be better choices for mismatch detection.

Table 1. Charge Transfer Resistance values for Matched and Single A-C Mismatched DNA Monolayer, the Influence of Different Cations.^a Unit: (k Ω cm²)

Metal ions	Matched			Mismatched			$\Delta\Delta R_{ct}$
	ds-DNA	M-DNA	ΔR_{ct}	ds-DNA	M-DNA	ΔR_{ct}	
Zn ²⁺	5.71(0.50)	3.40(0.70)	2.31(0.86)	4.38(0.52)	2.92(0.44)	1.46(0.68)	0.85(1.10)
Cd ²⁺	5.35(0.12)	0.79(0.16)	4.56(0.20)	4.08(0.17)	1.00(0.13)	3.09(0.21)	1.48(0.29)
Hg ²⁺	5.83(0.23)	0.55(0.39)	5.29(0.45)	4.08(0.23)	2.10(0.19)	1.98(0.30)	3.30(0.54)

^a The values in parentheses represent the standard deviations from several electrode measurements (n≥5).

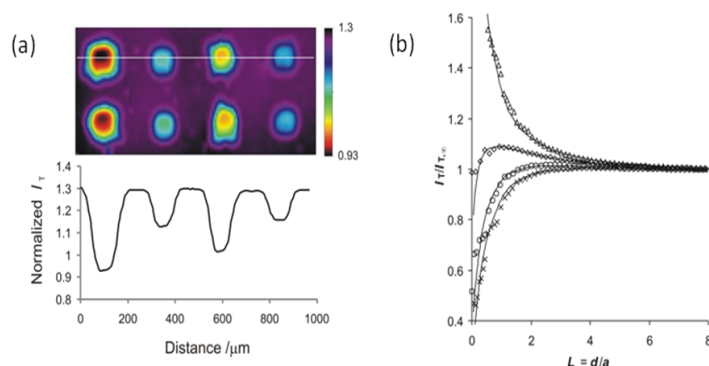


Fig. 3. (a) Typical SECM image and current profile recorded above DNA microarray in the presence of Zn^{2+} . Each sample was spotted twice from left to right in the following order: **A**, **B**, **C** and **D**. Experiment carried out in 1 mM $\text{K}_4\text{Fe}(\text{CN})_6$, 50 mM NaClO_4 , 20 mM Tris-ClO_4 (pH 8.6), with 25 μm Pt tip vs. Ag/AgCl , $E_T = 0.5$ V. (b) Typical normalized approach curves observed above individual ds-DNA spots for strands **A** (\times), **B** (\diamond), **C** (\circ) and **D** (Δ) measured in presence (b) of Zn^{2+} . Solid lines represent simulated approach curves for dimensionless rate constant in the absence of Zn^{2+} .

A typical SECM image and current profile recorded over a Zn^{2+} metallated ds-DNA microarray on a Au substrate have been shown in Fig 3a. Spots visible in the image correspond to **A**, **B**, **C** and **D** ds-DNA samples (from left to right). The second row of spots is identical to the first row. Two observations are immediately apparent: (a) there is a clear difference of the tip current, and thus the SECM image, for a fully matched ds-DNA film compared to the films formed from mismatched strands; (b) there are clear differences in the tip current as a function of A–C mismatch position. Although small, these differences are highly reproducible and are in line with results reported by Wain and Zhou.⁶ Presumably those differences in the tip current are due to the differences in the ability of the $[\text{Fe}(\text{CN})_6]^{3-/4-}$ redox probe to penetrate the film as reported before. Comparing with the case in the absence of Zn^{2+} (data now shown), significantly enhanced differences in the tip current were observed for the films of matched and mismatched ds-DNA. In addition, the tip currents were generally larger in the presence of Zn^{2+} .

Approach curves of DNA arrays were obtained from approaching the tip to the surface at the center of individual spots and shown in Fig 3b. In the presence of Zn^{2+} , significant differences in tip current were observed. Importantly, the tip current is significantly influenced by the position of the mismatch. Negative SECM feedback occurred for the matched ds-DNA **A** and the ds-DNA **C** containing a mismatch in the middle of the ds-DNA, while the tip current increased for **B**, and for **D** a partially positive feedback was observed. Experimental approach curves were further evaluated to estimate the kinetic parameters for the processes of the mediator regeneration at the substrate. A theoretical model was employed to evaluate heterogeneous electron transfer kinetics through the DNA films. Following values of apparent rate constant were obtained, $k^0 = 7.0 \pm 0.3 \times 10^{-5}$, $k^0 = 2.8 \pm 0.2 \times 10^{-4}$, $k^0 = 1.2 \pm 0.2 \times 10^{-4}$ and $k^0 = 1.3 \pm 0.3 \times 10^{-3} \text{ cm s}^{-1}$, for **A**, **B**, **C** and **D** respectively. The presence of Zn^{2+} causes a significant increase in the apparent rate constants for all four ds-DNA films as the presence of Zn^{2+} facilitates the diffusion of the redox mediator into the DNA films by reducing the electrostatic repulsion between the phosphate backbone and the redox probe. This is consistent with our previous EIS results. Importantly, the position of the mismatch influences the rate constant significantly, presumably since the position influences the film structure and that in turn influences the ability of the redox mediator to penetrate into the DNA film.

In conclusion, we evaluated the effects of various metal ions on the electrochemical impedance spectra of 25-mer ds-DNA films. Earlier work has shown that the addition of Zn^{2+} to films of ds-DNA decreases the charge transfer resistance R_{ct} for charge transfer from the ani-

onic redox probe $[\text{Fe}(\text{CN})_6]^{3-/4-}$ to an electrode surface.²⁷ This raised the question if there is anything special about Zn^{2+} or if other metals might be used instead potentially with even better results and give enhanced differences in the R_{ct} values. We chose the divalent transition metal ions Ni^{2+} , Cu^{2+} , Zn^{2+} , Cd^{2+} and Hg^{2+} . For all metal ions studied here, the presence of metal ions decreases the charge transfer resistance R_{ct} of ds-DNA films. The difference of ΔR_{ct} for the fully matched DNA and one single A-C mismatch DNA ($\Delta \Delta R_{ct}$) follows the order: $\text{Hg}^{2+} > \text{Cd}^{2+} > \text{Zn}^{2+}$, suggesting the Hg^{2+} might be a better choice for mismatch detection and might lead the way to optimizing the procedure for mismatch detection by EIS.

Furthermore, we have demonstrated that SECM can be employed to detect the presence and position of single-nucleotide mismatches in unlabeled ds-DNA films, by monitoring differences in the amperometric feedback current in the presence and absence of Zn^{2+} . Mathematical fitting of experimental approach curves to theory allowed us to assess the heterogeneous electron transfer kinetics through the DNA films in the absence and presence of Zn^{2+} . The presence of single-nucleotide mismatches caused an increase in electron transfer rate constant, presumably due to better penetration of the redox probe into the film. This is line with our above EIS results. Moreover, our results show an amplification of the differences in the rate constants between films made up of matched and mismatched ds-DNA after the addition of Zn^{2+} , which in principle may be employed to discriminate matched from mismatched ds-DNA and the position of the mismatch. Our results present a significant step forward towards the development of a rapid electrochemical method for detection of DNA mismatches and potentially allows the identification of positional parameters.

References:

1. J. Anastassopoulou, *J. Mol. Struct.*, 2003, **651-653**, 19-26.
2. Z. Hossain and F. Huq, *J. Inorg. Biochem.*, 2002, **90**, 97-105.
3. Y.-T. Long, C.-Z. Li, H.-B. Kraatz and J. S. Lee, *Biophys. J.*, 2003, **84**, 3218-3225.
4. X. Li, Y. Zhou, T. C. Sutherland, B. Baker, J. S. Lee and H.-B. Kraatz, *Anal. Chem.*, 2005, **77**, 5766-5769.
5. A. J. Bard and M. V. Mirkin., *Scanning Electrochemical Microscopy*, Marcel Dekker, New York, 2001.
6. J. Wain and F. Zhou. *Langmuir*, 2008, **24**, 5155–5160.

Western Nanofabrication Facility

University of Western Ontario
Physics & Astronomy Building Rm. 14
London, Ontario N6A 3K7

Dr. Bernie Kraatz, Facility Director
Ext. 81561 email: hhraatz@uwo.ca

Dr. Rick Glew, Laboratory Manager
Ext. 81458 Email: rglew@uwo.ca

Phone: 519-661-2111
Fax : 519-661-2033
www.uwo.ca/fab

Dr. Todd Simpson, Research Scientist
Ext. 86977 Email: tsimpson@uwo.ca

Tim Goldhawk, Laboratory Supervisor
Ext. 81457 Email: tim.goldhawk@uwo.ca

